

An Unusual Ligand in Copper Chemistry: Coordination Oligomers and Polymers Containing the  $[\{\text{CpMo}(\text{CO})_2\}_2(\mu, \eta^2\text{-Sb}_2)]$  Cluster

Hanh V. Ly, Masood Parvez, and Roland Roesler\*

Department of Chemistry, University of Calgary, Calgary, Alberta, Canada T2N 1N4

Received August 17, 2005

The coordination behavior of  $[\{\text{CpMo}(\text{CO})_2\}_2(\mu, \eta^2\text{-Sb}_2)]$  (**1**; Cp = cyclopentadiene) toward Cu(I) was investigated. Its reaction with CuX (X = Br, Cl, and I) produced oligomers or polymers of the general formula  $[\{\text{CpMo}(\text{CO})_2\}_2(\mu, \eta^2\text{-Sb}_2)(\mu\text{-CuX})]_n$ . While **2** (X = Cl,  $n = 2$ ) and **3** (X = Br,  $n = 2$ ) proved to be halogen-bridged dimers in both solution and solid state, the molecules of **4** (X = I,  $n = \infty$ ) self-assembled in the crystal forming a linear polymer with a Cu–I skeleton supported by Sb–Cu bonds. The reaction of **1** with  $\text{Cu}[\text{GaCl}_4]$  resulted in the formation of the ionic complex  $[\{\text{CpMo}(\text{CO})_2\}_2(\mu, \eta^2\text{-Sb}_2)]_4\text{Cu}_2[\text{GaCl}_4]_2$  (**5**). Its dication contains four  $[\{\text{CpMo}(\text{CO})_2\}_2(\mu, \eta^2\text{-Sb}_2)]$  ligands arranged around a Cu–Cu dumbbell. All new compounds were characterized using IR, electrospray ionization mass spectrometry,  $^1\text{H}$  NMR, elemental analysis, and single-crystal X-ray diffraction. The ligand was oxidized by both silver(I) and copper(II), and a cyclic voltammetric study revealed that **1** suffered irreversible reduction and oxidation in a dichloromethane solution at  $-2.04$  and  $0.10$  V, respectively, versus ferrocene.

## Introduction

The synthesis of molecular complexes containing substituent-free group 15 ligands,  $\text{E}_n$  (E = P, As, Sb, and Bi), has been a fertile area of research for a number of years.<sup>1</sup> In particular, the chemistry of the phosphorus and arsenic derivatives has been extensively studied because these compounds are easily accessible using elemental pnictogens as starting materials. Besides the sandwich and triple-decker sandwich complexes containing  $\pi$ -coordinating  $\text{E}_5$  and  $\text{E}_6$  ligands, tetrahedral clusters,  $\text{E}_n(\text{ML}_m)_{4-n}$ ,  $n = 1-3$ , are among the most common structural motifs in the chemistry of substituent-free group 15 ligands. The chemistry of the heavier antimony and bismuth analogues is much less developed in comparison to that of the phosphorus and arsenic derivatives. A few complexes containing  $\text{E}_2$  ligands have been structurally characterized for antimony<sup>2</sup> and

bismuth.<sup>3</sup> Complexes containing a linear<sup>4a,b</sup> or cyclic<sup>4c</sup>  $\text{Sb}_3$  unit have been reported as well, and also, an  $\text{Sb}_5$  ligand<sup>5</sup> has been stabilized in the coordination sphere of transition metals.  $\text{Sb}_3$  and  $\text{Bi}_3$  units exhibiting longer element–element bonds have also been observed as part of the polymetallic clusters.<sup>6</sup>

Complexes containing substituent-free  $\text{E}_n$  ligands generally have the ability to coordinate through the nonbonding electron pairs situated on the pnictogen atoms. A variety of compounds were obtained using the complexes  $[\text{MeC}(\text{CH}_2\text{-PPh}_2)_3\text{M}(\eta^3\text{-P}_3)]$  (M = Co, Rh, and Ir) as ligands for Cu(I), Ag(I), Au(I), and Hg(II).<sup>7</sup> More recently, complexes containing  $\text{P}_n$  units have been employed as ligands for the construc-

\* To whom correspondence should be addressed. E-mail: roesler@ucalgary.ca.

- (1) (a) Sacconi, L.; Di Vaira, M. *Angew. Chem., Int. Ed. Engl.* **1982**, *21*, 330–342; *Angew. Chem.* **1982**, *94*, 338–351. (b) Scherer, O. J. *Angew. Chem., Int. Ed. Engl.* **1990**, *29*, 1104–1122; *Angew. Chem.* **1990**, *102*, 1137–1155. (c) Scheer, M.; Herrmann, E. *Z. Chem.* **1990**, *30*, 41–55. (d) DiMaio, A.-J.; Rheingold, A. L. *Chem. Rev.* **1990**, *90*, 169–190. (e) Di Vaira, M.; Stoppioni, P. *Coord. Chem. Rev.* **1992**, *120*, 259–279. (f) Whitmire, K. H. *Adv. Organomet. Chem.* **1998**, *42*, 1–145. (g) Scherer, O. J. *Acc. Chem. Res.* **1999**, *32*, 751–762.
- (2) (a) Huttner, G.; Weber, U.; Sigwarth, B.; Scheidsteiger, O. *Angew. Chem., Int. Ed. Engl.* **1982**, *21*, 215–216; *Angew. Chem.* **1982**, *94*, 210. (b) Rheingold, A. L.; Harper, J. R. *J. Organomet. Chem.* **1990**, *390*, C36.

- (3) (a) Huttner, G.; Weber, U.; Zsolnai, L. *Z. Naturforsch., B: Chem. Sci.* **1982**, *37*, 707–710. (b) Ang, H. G.; Hay, C. M.; Johnson, B. F. G.; Lewis, J.; Raithby, P. R.; Whitton, A. J. *J. Organomet. Chem.* **1987**, *330*, C5–C11. (c) Plöchl, K.; Huttner, G.; Zsolnai, L. *Angew. Chem., Int. Ed. Engl.* **1989**, *28*, 446–447; *Angew. Chem.* **1989**, *101*, 482. (d) Evans, W. J.; Gonzales, S. L.; Ziller, J. W. *J. Am. Chem. Soc.* **1991**, *113*, 9880–9882. (e) Clegg, W.; Compton, N. A.; Errington, R. J.; Fisher, G. A.; Norman, N. C.; Marder, T. B. *J. Chem. Soc., Dalton Trans.* **1991**, 2887–2895.
- (4) (a) Evans, W. J.; Gonzales, S. L.; Ziller, J. W. *J. Chem. Soc., Chem. Commun.* **1992**, 1138–1139. (b) Wagner, C.; Merzweiler, K. *Phosphorus, Sulfur Silicon Relat. Elem.* **2001**, *168–169*, 199–202. (c) Breunig, H. J.; Rösler, R.; Lork, E. *Angew. Chem., Int. Ed. Engl.* **1997**, *36*, 2819–2821; *Angew. Chem.* **1997**, *109*, 2941–2942.
- (5) Breunig, H. J.; Roesler, R.; Burford, N. *Angew. Chem., Int. Ed.* **2000**, *39*, 4148–4150; *Angew. Chem.* **2000**, *112*, 4320–4322.
- (6) (a) Gröer, T.; Scheer, M. *Organometallics* **2000**, *19*, 3683–3691. (b) Gröer, T.; Palm, T.; Scheer, M. *Eur. J. Inorg. Chem.* **2000**, 2591–2595.

tion of self-assembled mono- and bidimensional polymers involving monovalent  $d^{10}$  metal cations. The reaction of  $[\{\text{CpMo}(\text{CO})_2\}_2(\mu, \eta^2\text{-P}_2)]$  (Cp = cyclopentadiene) with  $\text{AgNO}_3$  or  $\text{CuX}$  ( $X = \text{Cl}, \text{Br}, \text{and I}$ ) resulted in the formation of monodimensional polymers.<sup>8a,d</sup> Further studies were conducted with the sandwich complex  $[\text{Cp}^*\text{Fe}(\eta^5\text{-P}_5)]$ , which produced mono- and bidimensional coordination polymers in reaction with different Cu(I) halides.<sup>8b</sup> The same synthon was used for the self-assembly of a spectacular spherical fullerene-like structure having a  $[\text{Cp}^*\text{Fe}(\eta^5\text{-P}_5)]_{12}(\text{CuCl})_{15}$  framework.<sup>8c</sup> In contrast to the polymers described above, the latter complex dissolved in organic solvents without decomposition. Finally, the formation of cyclic antimony ligands has been observed in the reaction of  $\text{CuCl}$  with  $\text{LiSb}(\text{SiMe}_3)_2$  in the presence of a chelating phosphine. The resulting cluster contained in situ formed  $\text{Sb}_3$  units coordinated to copper.<sup>9</sup>

The formation of supramolecular aggregates through self-organization has received considerable attention in recent years.<sup>10</sup> The self-organization process proved to be very sensitive to numerous factors such as the nature of the coordination site, the structure of the bridging ligand, the geometric preferences of the metal ions, and the solvent. We were interested in the potential of tetrahedral clusters containing substituent-free antimony ligands as precursors for the generation of self-assembled structures, and we report here the synthesis and structural characterization of oligomeric and polymeric  $[\{\text{CpMo}(\text{CO})_2\}_2(\mu, \eta^2\text{-Sb}_2)]\text{-CuX}$  adducts ( $X = \text{Cl}, \text{Br}, \text{I}, \text{and GaCl}_4$ ). To our knowledge, the coordination chemistry of complexes containing  $\text{Sb}_n$  ligands has not yet been investigated. Complexes containing  $\text{Sb}_3$  units, however, displayed interesting associations through  $\text{Sb}\cdots\text{Sb}$  interactions in the solid state.<sup>4c</sup>

## Experimental Section

**General Data.** All operations were performed under an argon atmosphere using standard Schlenk and glovebox techniques. Solvents were dried and deoxygenated,  $\text{SbCl}_3$  was sublimed, and Mg metal was activated in situ using dibromoethane prior to use.

- (7) (a) Ceconi, F.; Ghilardi, C. A.; Midollini, S.; Orlandini, A. *J. Chem. Soc., Chem. Commun.* **1982**, 229–230. (b) Ceconi, F.; Ghilardi, C. A.; Midollini, S.; Orlandini, A. *Angew. Chem., Int. Ed. Engl.* **1983**, *22*, 554–555; *Angew. Chem.* **1983**, *95*, 554–555. (c) Di Vaira, M.; Rovai, D.; Stoppioni, P. *Polyhedron* **1990**, *9*, 2477–2481. (d) Di Vaira, M.; Stoppioni, P.; Peruzzini, M. *J. Chem. Soc., Dalton Trans.* **1990**, 109–113. (e) Di Vaira, M.; Ehses, M. P.; Peruzzini, M.; Stoppioni, P. *Polyhedron* **1999**, *18*, 2331–2336.
- (8) (a) Bai, J.; Virovets, A. V.; Scheer, M. *Angew. Chem., Int. Ed.* **2002**, *41*, 1737–1740; *Angew. Chem.* **2002**, *114*, 1808–1811. (b) Bai, J.; Leiner, E.; Scheer, M. *Angew. Chem., Int. Ed.* **2002**, *41*, 783–786; *Angew. Chem.* **2002**, *114*, 820–823. (c) Bai, J.; Virovets, A. V.; Scheer, M. *Science* **2003**, *300*, 781–783. (d) Scheer, M.; Gregoriades, L.; Bai, J.; Sierka, M.; Brunklaus, G.; Eckert, H. *Chem.—Eur. J.* **2005**, *11*, 2163–2169.
- (9) Besinger, J.; Treptow, J.; Fenske, D. *Z. Anorg. Allg. Chem.* **2002**, *628*, 512–515.
- (10) (a) Stang, P. J.; Olenyuk, B. *Acc. Chem. Res.* **1997**, *30*, 502–518. (b) Lindoy, L. F.; Atkinson, I. M. *Self-assembly in Supramolecular Systems*; Royal Society of Chemistry: Cambridge, U.K., 2000. (c) Fujita, M., Ed. *Molecular Self-Assembly Organic Versus Inorganic Approaches*; Springer: Berlin, Germany, 2000. (d) Seidel, S. R.; Stang, P. J. *Acc. Chem. Res.* **2002**, *35*, 972–983. (e) Keizer, H. M.; Sijbesma, R. P. *Chem. Soc. Rev.* **2005**, *34*, 226–234.

$\text{Cu}[\text{GaCl}_4]^{11}$  and cyclo-*t*-Bu<sub>4</sub>Sb<sub>4</sub><sup>12</sup> were prepared according to reported procedures. The NMR spectra were collected on a Bruker AM-200 spectrometer. IR spectra were acquired using KBr pellets on a Nicolet Nexus 470 spectrophotometer in the 4000–400  $\text{cm}^{-1}$  region. Mass spectra and elemental analyses were performed by the Analytical Instrumentation Laboratory, Department of Chemistry, University of Calgary.

**Synthesis of  $[\{\text{CpMo}(\text{CO})_2\}_2(\mu, \eta^2\text{-Sb}_2)]$ , **1**.** A mixture of cyclo-*t*-Bu<sub>4</sub>Sb<sub>4</sub> (1 g, 1.39 mmol) and  $[\text{CpMo}(\text{CO})_3]_2$  (0.684 g, 1.39 mmol) was stirred in decaline (50 mL) at 120 °C for 1 h and subsequently at 190 °C for another 2 h. The reaction mixture was allowed to cool to room temperature, and the solvent was removed in vacuo leaving behind a dark residue that was washed with hexane and extracted with toluene ( $2 \times 50$  mL). Upon evaporation of the solvent, dark red crystals of **1** (584 mg, 0.862 mmol, 62%) were obtained. The analytical data were in agreement with the reported values.<sup>2b,5</sup> <sup>1</sup>H NMR ( $\text{C}_6\text{D}_6$ , 25 °C,  $\delta$ ): 5.09 (s,  $\text{C}_5\text{H}_5$ ). IR ( $\text{cm}^{-1}$ ): 1919, 1886 [ $\nu(\text{CO})$ ].

**Synthesis of  $[\{\text{CpMo}(\text{CO})_2\}_2(\mu, \eta^2\text{-Sb}_2)(\mu\text{-CuCl})]_2$ , **2**.** A solution of  $\text{CuCl}$  (17 mg, 0.177 mmol) in  $\text{CH}_3\text{CN}$  (3 mL) was layered over a solution of **1** (60 mg, 0.088 mmol) in  $\text{CH}_2\text{Cl}_2$  (10 mL). Dark red crystals of **2** (60 mg, 0.077 mmol, 87%) were deposited after 1 week at room temperature and were isolated.

Elem anal. Calcd for  $\text{C}_{28}\text{H}_{20}\text{Cl}_2\text{Cu}_2\text{Mo}_4\text{O}_8\text{Sb}_4$  (%): C, 21.65; H, 1.30. Found: C, 21.73; H, 1.05. <sup>1</sup>H NMR ( $\text{CD}_2\text{Cl}_2$ , 25 °C,  $\delta$ ): 5.134 (s,  $\text{C}_5\text{H}_5$ ). IR ( $\text{cm}^{-1}$ ): 1933, 1896, 1868 [ $\nu(\text{CO})$ ]. ESI-MS ( $m/z$ , relative intensity): 1517(5) [ $\text{M} - \text{Cl}$ ]<sup>+</sup>, 1419(20)  $[\{\{\text{CpMo}(\text{CO})_2\}_2\text{Sb}_2\text{Cu}\}]^+$ , 1194(75)  $[\{\text{Cp}_2\text{Mo}_2\text{Sb}_2\}_2\text{Cu}]^+$ , 971(15)  $[\text{Cp}_2\text{Mo}_3\text{-Sb}_4\text{Cu}]^+$ , 629(100)  $[(\text{CpMoSb})_2\text{Cu}]^+$ .

**Synthesis of  $[\{\text{CpMo}(\text{CO})_2\}_2(\mu, \eta^2\text{-Sb}_2)(\mu\text{-CuBr})]_2$ , **3**.** A solution of  $\text{CuBr}$  (25 mg, 0.177 mmol) in  $\text{CH}_3\text{CN}$  (3 mL) was layered over a solution of **1** (60 mg, 0.088 mmol) in  $\text{CH}_2\text{Cl}_2$  (10 mL). The formation of dark red crystals of **3** (50 mg, 0.061 mmol, 70%) was induced through the storage of the solution at  $-30$  °C for 2 days, and the crystals were isolated by decanting off the mother liquor.

Elem anal. Calcd for  $\text{C}_{28}\text{H}_{20}\text{Br}_2\text{Cu}_2\text{Mo}_4\text{O}_8\text{Sb}_4$  (%): C, 20.48; H, 1.23. Found: C, 20.76; H, 1.34. <sup>1</sup>H NMR ( $\text{CD}_2\text{Cl}_2$ , 25 °C,  $\delta$ ): 5.169 (s,  $\text{C}_5\text{H}_5$ ). IR ( $\text{cm}^{-1}$ ): 1939, 1897, 1866 [ $\nu(\text{CO})$ ]. ESI-MS ( $m/z$ , relative intensity): 1564(30) [ $\text{M} - \text{Br}$ ]<sup>+</sup>, 1419(85)  $[\{\{\text{CpMo}(\text{CO})_2\}_2\text{Sb}_2\text{Cu}\}]^+$ , 1194(100)  $[\{\text{Cp}_2\text{Mo}_2\text{Sb}_2\}_2\text{Cu}]^+$ , 971(30)  $[\text{Cp}_2\text{-Mo}_3\text{Sb}_4\text{Cu}]^+$ , 628(50)  $[(\text{CpMoSb})_2\text{Cu}]^+$ .

**Synthesis of  $[\{\text{CpMo}(\text{CO})_2\}_2(\mu, \eta^2\text{-Sb}_2)(\mu\text{-CuI})]_2$ , **4**.** A solution of  $\text{CuI}$  (34 mg, 0.177 mmol) in  $\text{CH}_3\text{CN}$  (3 mL) was added to a solution of **1** (60 mg, 0.088 mmol) in  $\text{CH}_2\text{Cl}_2$  (10 mL). The slow evaporation of the solvent produced dark red crystals of **4** (30 mg, 0.068 mmol, 77%).

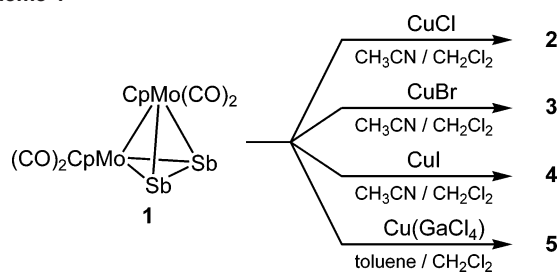
Elem anal. Calcd for  $\text{C}_{28}\text{H}_{20}\text{I}_2\text{Cu}_2\text{Mo}_4\text{O}_8\text{Sb}_4$  (%): C, 19.15; H, 1.15; N, 0.40. Found: C, 19.44; H, 1.11; N, 0.71. <sup>1</sup>H NMR ( $\text{CD}_2\text{-Cl}_2$ , 25 °C,  $\delta$ ): 5.107 (s,  $\text{C}_5\text{H}_5$ ), 1.974 (s,  $\text{CH}_3\text{CN}$ ). IR ( $\text{cm}^{-1}$ ): 1941, 1908, 1888, 1871 [ $\nu(\text{CO})$ ]. ESI-MS ( $m/z$ , relative intensity): 1610(10) [ $\text{M} - \text{I}$ ]<sup>+</sup>, 1419(60)  $[\{\{\text{CpMo}(\text{CO})_2\}_2\text{Sb}_2\text{Cu}\}]^+$ , 1194(80)  $[\{\text{Cp}_2\text{Mo}_2\text{Sb}_2\}_2\text{Cu}]^+$ , 971(30)  $[\text{Cp}_2\text{Mo}_3\text{Sb}_4\text{Cu}]^+$ , 629(100)  $[(\text{CpMoSb})_2\text{Cu}]^+$ .

**Synthesis of  $[\{\text{CpMo}(\text{CO})_2\}_2(\mu, \eta^2\text{-Sb}_2)]_4\text{Cu}_2[\text{GaCl}_4]_2$ , **5**.** A solution of  $\text{Cu}[\text{GaCl}_4]$  (20 mg, 0.072 mmol) in toluene (5 mL) was layered over a solution of **1** (50 mg, 0.073 mmol) in  $\text{CH}_2\text{Cl}_2$  (10 mL). Diffusion was completed after 1 week, and the orange-brown

- (11) Schmidbaur, H.; Bublak, W.; Huber, B.; Reber, G.; Müller, G. *Angew. Chem., Int. Ed. Engl.* **1986**, *25*, 1089–1090; *Angew. Chem.* **1986**, *98*, 1108–1109.

- (12) (a) Issleib, K.; Hamann, B.; Schmidt, L. *Z. Anorg. Allg. Chem.* **1965**, *339*, 298–303. (b) Breunig, H. J. *Z. Naturforsch., B: Chem. Sci.* **1978**, *33*, 242–243. (c) Breunig, H. J.; Pawlik, J. *Z. Anorg. Allg. Chem.* **1995**, *621*, 817–822. (d) Breunig, H. J.; Rösler, R.; Lork, E. *Z. Anorg. Allg. Chem.* **1999**, *625*, 1619–1623.

## Scheme 1



needles of **5** (40 mg, 0.056 mmol, 77%) were collected. Better quality single crystals of  $\mathbf{5} \cdot 3\text{C}_6\text{H}_6$  were obtained by the same procedure, using a benzene solution of  $\text{Cu}[\text{GaCl}_4]$  in an H tube.

Elem anal. Calcd for  $\text{C}_{74}\text{H}_{58}\text{Cl}_8\text{Cu}_2\text{Ga}_2\text{Mo}_8\text{O}_{16}\text{Sb}_8$  (%): C, 25.43; H, 1.67. Found: C, 26.07; H, 1.74.  $^1\text{H}$  NMR ( $\text{CD}_2\text{Cl}_2$ , 25  $^\circ\text{C}$ ,  $\delta$ ): 5.27 (s,  $\text{C}_5\text{H}_5$ ). IR ( $\text{cm}^{-1}$ ): 2011, 1966, 1941, 1911, 1899, 1889 [ $\nu(\text{CO})$ ]. ESI-MS ( $m/z$ , relative intensity): 1419(15) [ $\{\{\text{CpMo}(\text{CO})_2\}_2\text{Sb}_2\}_2\text{Cu}\}^+$ ], 1194(100) [ $\{\text{Cp}_2\text{Mo}_2\text{Sb}_2\}_2\text{Cu}\}^+$ ], 971(10) [ $\text{Cp}_2\text{Mo}_3\text{Sb}_4\text{Cu}\}^+$ ], 629(50) [ $\{\text{CpMoSb}\}_2\text{Cu}\}^+$ ].

**X-ray Crystallography.** Single crystals of **2**, **3**, **4**, and **5** were coated with Paratone 8277 oil (Exxon) and mounted onto thin glass fibers. All measurements were made on a Nonius Kappa charge-coupled device diffractometer, using graphite monochromated  $\text{Mo K}\alpha$  radiation ( $\lambda = 0.71073 \text{ \AA}$ ). The data were collected<sup>13</sup> at a temperature of 173(2) K using  $\varphi$  and  $\omega$  scans and corrected for Lorentz and polarization effects and for absorption using the multiscan method.<sup>14</sup>

The structures were solved by direct methods<sup>15</sup> and expanded using Fourier techniques.<sup>16</sup> The non-hydrogen atoms were refined anisotropically. Hydrogen atoms were included at geometrically idealized positions and were not refined. The final cycles of the full-matrix least-squares refinement using SHELXL97<sup>17</sup> converged with unweighted and weighted agreement factors, R and wR (all data), respectively, and goodness of fit on  $F^2$ . The weighting scheme was based on counting statistics, and the final difference map was essentially featureless. The figures were plotted with the aid of Diamond.<sup>18</sup>

**Cyclovoltammetry of 1.** The measurements were performed in the absence of oxygen, in anhydrous dichloromethane, at an analyte concentration of 1 mM, and in the presence of 0.1 M [ $n\text{-Bu}_4\text{P}$ ] $\text{PF}_6$  as a supporting electrolyte. An EG&G 283 potentiostat was used at scan rates of 200 and 1000  $\text{mV} \cdot \text{s}^{-1}$ . The three-electrode cell had a platinum disk working electrode, a platinum wire auxiliary electrode, and a silver wire pseudo-reference electrode. [ $\text{Cp}_2\text{Co}$ ] $^{0/+1}$  with  $E^0 = -1.33 \text{ V}$  versus ferrocene and  $-0.87 \text{ V}$  versus a saturated calomel electrode was used as an internal standard.

## Results and Discussion

The ligand **1** was prepared using a modification of the published procedures.<sup>2b,4c</sup> At a higher reaction temperature, the more stable **1** was obtained as the only soluble antimony-

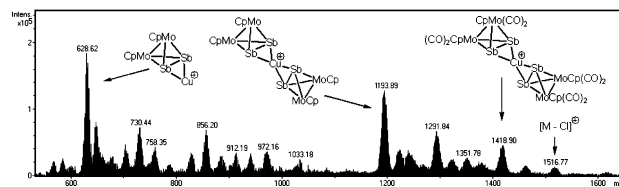


Figure 1. ESI-MS spectrum of **2** in the 550–1650  $m/z$  range.

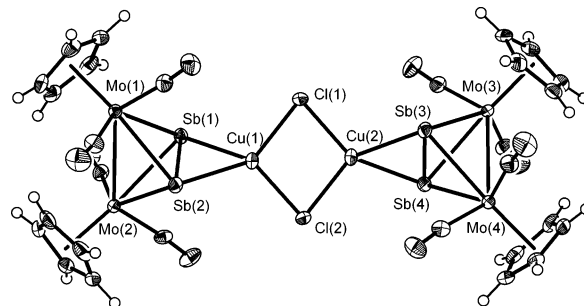


Figure 2. View of one of the two independent dimeric units of **2**.

containing product in 62% yield. The adducts **2**, **3**, and **4** (Scheme 1) were isolated as dark red crystalline solids after the diffusion-controlled mixing of the reagents. The solubility of the resulting complexes in organic solvents ( $\text{CH}_3\text{CN}$ ,  $\text{CH}_2\text{Cl}_2$ , and  $\text{C}_6\text{H}_6$ ) increases with the polarity of the solvent and the atomic number of the halogen. While the chloro derivative is nearly insoluble in a 2:1  $\text{CH}_2\text{Cl}_2/\text{CH}_3\text{CN}$  mixture, the iodo derivatives dissolve well in the same mixture producing a dark red solution. This sets these complexes apart from the  $\text{CuX}$  ( $X = \text{Cl}$ ,  $\text{Br}$ , and  $\text{I}$ ) adducts of the phosphorus analogue of **1**, which are insoluble in common solvents.<sup>8a,d</sup> The identities of the compounds were determined by single-crystal X-ray crystallographic analysis and confirmed using elemental analysis, IR spectroscopy,  $^1\text{H}$  NMR, and electrospray ionization mass spectrometry (ESI-MS).

For all adducts, the IR spectra showed broad absorptions in the carbonyl region, corresponding to the stretching vibrations of the terminal CO groups in ligand **1**. The absorptions fell between 1941 and 1866  $\text{cm}^{-1}$ , close to the values assigned to the free ligand (1919 and 1886  $\text{cm}^{-1}$ ). The  $^1\text{H}$  NMR spectra displayed the expected resonance characteristic to the cyclopentadienyl group. In the positive-ion ESI-MS spectrum of **2** in acetonitrile (Figure 1), the highest  $m/z$  value (1517) corresponded to the fragment [ $\{\{\text{CpMo}(\text{CO})_2\}_2\text{Sb}_2\}_2\text{Cu}_2\text{Cl}\}^+$ ], which resulted through the loss of one  $\text{Cl}^-$  ion from the dimer [ $\{\{\text{CpMo}(\text{CO})_2\}_2\text{Sb}_2\}_2\text{-(CuCl)}_2$ ]. The further loss of  $\text{CuCl}$  produced the ion [ $\{\{\text{CpMo}(\text{CO})_2\}_2\text{Sb}_2\}_2\text{Cu}\}^+$ , containing a four-coordinated  $\text{Cu}(\text{I})$  at  $m/z = 1419$ . The successive loss of eight CO ligands from this fragment produced the ion [ $\{\text{Cp}_2\text{Mo}_2\text{Sb}_2\}_2\text{Cu}\}^+$  with  $m/z = 1194$ . Ions resulting from the successive loss of  $\text{Cp}_2\text{Mo}$ , each of the antimony atoms, and finally molybdenum could also be identified. The ESI-MS spectra of **3** and **4** showed the same fragmentation patterns as the one observed for **2**, with all signals displaying the typical wide isotopic distribution.

Crystal structure determinations (Table 1) showed that compounds **2** and **3** (Figure 2) are isomorphous, and

- (13) Otwinowski, Z.; Minor, W. *Methods Enzymol.* **1997**, *276*, 307–326.  
 (14) Hooft, R. *COLLECT*; Nonius BV: Delft, The Netherlands, 1998.  
 (15) Altomare, A.; Casciarano, M.; Giacovazzo, C.; Guagliardi, A. *J. Appl. Crystallogr.* **1993**, *26*, 343.  
 (16) Beurskens, P. T.; Admiraal, G.; Beurskens, G.; Bosman, W. P.; de Gelder, R.; Israel, R.; Smits, J. M. M. *The DIRDIF-94 program system*; Technical Report of the Crystallography Laboratory; University of Nijmegen: Nijmegen, The Netherlands, 1994.  
 (17) Sheldrick, G. M. *SHELXL97*; University of Göttingen: Göttingen, Germany, 1997.  
 (18) *DIAMOND*, version 3.0; Visual Crystal Structure Information System; Crystal Impact: Bonn, Germany, 1997–2005.

**Table 1.** Selected Data and Structure Refinement for **2**, **3**, **4**, and **5**

	<b>2</b>	<b>3</b>	<b>4</b>	<b>5</b>
empirical formula	C <sub>28</sub> H <sub>20</sub> Cl <sub>2</sub> Cu <sub>2</sub> Mo <sub>4</sub> -O <sub>8</sub> Sb <sub>4</sub>	C <sub>28</sub> H <sub>20</sub> Br <sub>2</sub> Cu <sub>2</sub> Mo <sub>4</sub> -O <sub>8</sub> Sb <sub>4</sub>	C <sub>28</sub> H <sub>20</sub> Cu <sub>2</sub> I <sub>2</sub> Mo <sub>4</sub> -O <sub>8</sub> Sb <sub>4</sub> ·0.5CH <sub>3</sub> CN	C <sub>74</sub> H <sub>58</sub> Cl <sub>8</sub> Cu <sub>2</sub> Ga <sub>2</sub> -Mo <sub>8</sub> O <sub>16</sub> Sb <sub>8</sub>
formula weight	1553.18	1642.10	1756.61	3494.84
crystal system	triclinic	triclinic	triclinic	orthorhombic
space group	<i>P</i> $\bar{1}$	<i>P</i> $\bar{1}$	<i>P</i> $\bar{1}$	<i>P</i> 2 <sub>1</sub> 2 <sub>1</sub>
unit cell dimensions	<i>a</i> = 15.068(2) Å <i>b</i> = 15.241(3) Å <i>c</i> = 17.156(4) Å $\alpha$ = 89.37(2)° $\beta$ = 88.705(13)° $\gamma$ = 69.221(11)°	<i>a</i> = 15.028(3) Å <i>b</i> = 15.249(3) Å <i>c</i> = 17.491(4) Å $\alpha$ = 88.793(9)° $\beta$ = 88.916(8)° $\gamma$ = 70.764(16)°	<i>a</i> = 10.006(2) Å <i>b</i> = 14.851(3) Å <i>c</i> = 14.926(3) Å $\alpha$ = 107.859(11)° $\beta$ = 104.645(12)° $\gamma$ = 97.191(11)°	<i>a</i> = 16.167(2) Å <i>b</i> = 21.869(3) Å <i>c</i> = 26.715(4) Å $\alpha$ = 90° $\beta$ = 90° $\gamma$ = 90°
volume	3682.7(12) Å <sup>3</sup>	3783.3(14) Å <sup>3</sup>	1992.4(7) Å <sup>3</sup>	9445(2) Å <sup>3</sup>
Z	4	4	2	4
absorption coefficient	5.517 mm <sup>-1</sup>	7.341 mm <sup>-1</sup>	6.52 mm <sup>-1</sup>	4.55 mm <sup>-1</sup>
crystal size	0.20 × 0.18 × 0.18 mm	0.20 × 0.12 × 0.10 mm	0.06 × 0.06 × 0.04 mm	0.36 × 0.24 × 0.07 mm
independent reflns	20 980 ( <i>R</i> <sub>int</sub> = 0.0426)	17 180 ( <i>R</i> <sub>int</sub> = 0.0659)	9047 ( <i>R</i> <sub>int</sub> = 0.043)	9008 ( <i>R</i> <sub>int</sub> = 0.032)
data/restraints/parameters	20 980/0/865	17 180/0/865	9047/0/445	9008/0/1064
final R indices [ <i>I</i> > 2σ( <i>I</i> )]	R1 = 0.0331 wR2 = 0.0801	R1 = 0.0421 wR2 = 0.0644	R1 = 0.038 wR2 = 0.071	R1 = 0.036 wR2 = 0.079

**Table 2.** Selected Bond Lengths (Å) and Bond Angles (deg) for **2** and **3**<sup>a</sup>

	X = Cl ( <b>2</b> )	X = Br ( <b>3</b> )
Cu–X	2.2797(17)–2.3067(17)	2.3995(13)–2.4323(14)
Sb–Cu	2.5607(10)–2.5760(10)	2.5889(12)–2.6071(13)
Cu···Cu	2.9158(12), 2.9607(12)	2.9403(14), 2.9448(14)
Sb–Sb	2.7534(7)–2.7649(6)	2.7583(9)–2.7642(8)
Sb–Mo	2.7351(7)–2.8667(8)	2.7477(9)–2.8807(11)
Mo–Mo	3.0957(8)–3.1321(10)	3.1357(10)–3.1578(11)
Cu–X–Cu	78.95(6)–80.86(6)	74.92(4)–75.36(4)
X–Cu–X	99.20(6)–101.27(6)	104.08(4)–105.60(4)
Sb–Cu–Sb	64.42(3)–65.33(2)	63.94(3)–64.48(3)
Cu–Sb–Sb	57.31(2)–57.86(2)	57.69(3)–58.12(3)

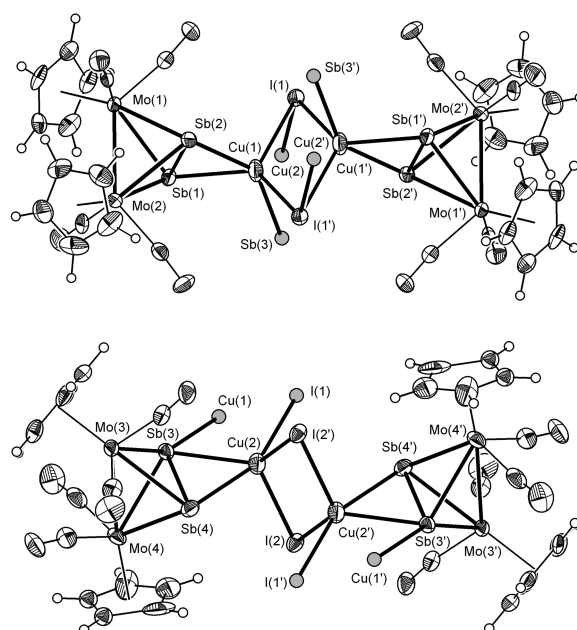
<sup>a</sup>For comparison, the free ligand **1** exhibits the following metric parameters: Sb–Sb, 2.678(1); Sb–Mo, 2.762(1) and 2.854(1); and Mo–Mo, 3.114(1).<sup>2b</sup>

consequently, they will be discussed together. Selected bond lengths and angles are summarized in Table 2. The structures revealed that these adducts form dimers in the solid state. The framework of **2** consists of two copper atoms bridged by two chloride units, forming a planar Cu<sub>2</sub>Cl<sub>2</sub> four-membered ring. Each copper center is coordinated by both of the antimony atoms of a [CpMo(CO)<sub>2</sub>]<sub>2</sub>Sb<sub>2</sub> ligand, achieving a distorted tetrahedral coordination environment. The Sb–Cu–Sb angles [63.94(3)–65.33(2)°] are significantly smaller than those observed in the related complexes, [(Ph<sub>3</sub>Sb)<sub>2</sub>Cu( $\mu$ -X)]<sub>2</sub>, containing nonchelating stibine ligands [average (av.) angle = 112.62°].<sup>19</sup> The Sb<sub>2</sub>Cu planes are not perpendicular to the Cu<sub>2</sub>Cl<sub>2</sub> plane but tilted, forming dihedral angles of 49.8–63.7°.

The Cu–X bonds in **2** and **3** are intermediate in length between the bridging Cu–X bonds in [(Ph<sub>3</sub>Sb)<sub>2</sub>Cu( $\mu$ -X)]<sub>2</sub> [2.326(2)–2.367(2) Å for X = Cl and 2.452(2)–2.488(3) Å for X = Br]<sup>19</sup> and the terminal Cu–X bond in [(Ph<sub>3</sub>Sb)<sub>3</sub>CuX] [2.235(5) and 2.366(3) Å, respectively].<sup>20,21</sup> Despite the shorter Cu–X bonds, the Cu···Cu distances in **2** and **3** are larger than in the [(Ph<sub>3</sub>Sb)<sub>2</sub>Cu( $\mu$ -X)]<sub>2</sub> analogues

(by ca. 0.09 Å for Cl and 0.13 Å for Br), resulting in a widening of the Cu–X–Cu angles by 5°. Predictably, the Cu–Sb bond lengths in **2** and **3** are longer than in [(Ph<sub>3</sub>Sb)<sub>2</sub>Cu( $\mu$ -X)]<sub>2</sub> [2.5280(9)–2.5392(9) Å for X = Cl and 2.534(2)–2.547(2) Å for X = Br].

Clusters containing a cyclic P<sub>3</sub> unit demonstrated the ability to chelate copper, gold, and mercury [P–P ligand bite, 2.257(3)–2.37(1) Å in complexes].<sup>7</sup> The shorter P–P distance [2.075(2)–2.080(2) Å] likely prevents the phosphorus analogue of **1** from being an efficient chelating ligand for those metals. Therefore, the phosphorus cluster prefers to coordinate in a bridging fashion, generating linear polymers with both CuCl and CuBr.<sup>8a,d</sup> The wide Sb–Sb bite (ca. 2.76 Å), however, enables **1** to be an efficient chelating ligand. The copper–halogen bonds in **2** and **3** are about 0.6 Å longer than in the polymeric analogues containing [CpMo(CO)<sub>2</sub>]<sub>2</sub>P<sub>2</sub> as a consequence of the expected

**Figure 3.** View of the two dimeric components in the polymeric structure of **4** showing the connecting atoms from neighboring dimers.

(19) Bowmaker, G. A.; Hart, R. D.; White, A. H. *Aust. J. Chem.* **1997**, *50*, 567–576.

(20) Bowmaker, G. A.; Hart, R. D.; de Silva, E. N.; Skelton, B. W.; White, A. H. *Aust. J. Chem.* **1997**, *50*, 621–626.

(21) Rheingold, A. L.; Fountain, M. E. *J. Crystallogr. Spectrosc. Res.* **1984**, *14*, 549–557.

**Table 3.** Selected Bond Lengths (Å) and Angles (deg) for **4**·0.5CH<sub>3</sub>CN

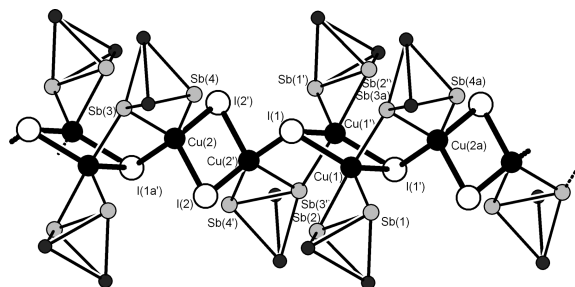
Cu(1)–I(1)	2.6341(11)	Cu(2)–I(2)	2.6898(10)
Cu(1)–I(1')	2.6329(10)	Cu(2)–I(2')	2.6948(11)
Cu(1)–Sb(3)	2.9361(14)	Cu(2)–I(1)	2.7990(13)
Cu(1)–Sb(1)	2.6237(10)	Cu(2)–Sb(3)	2.6944(11)
Cu(1)–Sb(2)	2.7206(13)	Cu(2)–Sb(4)	2.7335(13)
Cu(1)···Cu(1')	2.6781(17)	Cu(2)···Cu(2')	2.9745(18)
Sb(1)–Sb(2)	2.7388(9), 2.7487(9)	Mo–Mo	3.1478(9)–3.1917(9)
Sb–Mo	2.7619(10)–2.8808(9)		
Sb(2)–Cu(1)–Sb(3)	146.95(4)	I(1)–Cu(2)–Sb(4)	158.36(4)
I(1')–Cu(1)–I(1)	118.88(3)	I(2)–Cu(2)–I(2')	112.94(4)
I(1)–Cu(1)–Sb(1)	111.30(4)	I(2)–Cu(2)–Sb(3)	114.70(4)
I(1')–Cu(1)–Sb(1)	128.99(4)	I(2')–Cu(2)–Sb(3)	125.12(4)
I(1')–Cu(1)–Sb(2)	93.37(4)	I(2')–Cu(2)–Sb(4)	90.42(4)
I(1)–Cu(1)–Sb(2)	107.87(4)	I(2)–Cu(2)–Sb(4)	94.42(4)
Sb(1)–Cu(1)–Sb(2)	61.87(3)	Sb(3)–Cu(2)–Sb(4)	60.60(3)
I(1')–Cu(1)–Sb(3)	92.58(4)	I(2')–Cu(2)–I(1)	95.63(3)
I(1)–Cu(1)–Sb(3)	97.46(4)	I(2)–Cu(2)–I(1)	102.23(4)
Sb(1)–Cu(1)–Sb(3)	89.56(4)	Sb(3)–Cu(2)–I(1)	99.44(4)
Cu(1)–I(1)–Cu(1')	61.12(3)	Cu(2)–I(2)–Cu(2')	67.06(4)
Cu(1)–I(1)–Cu(2)	77.64(4)	Cu(1')–I(1)–Cu(2)	109.90(4)
Cu(1)–Sb(3)–Cu(2)	74.37(3)	Cu(1)–Sb(3)–Sb(4)	132.48(3)
Cu–Sb–Sb	57.33(3)–60.80(3)		

weaker electron-donating ability of antimony in comparison to that of phosphorus.

The only notable change in the structure of the cluster ligand **1** upon coordination is the elongation of the Sb–Sb bonds by 3% (ca. 0.08 Å). This change is not surprising given the increase in the coordination number for antimony from 3 to 4. The Sb–Sb bonds are still shorter than the typical Sb–Sb single bonds, which average 2.83 Å in cyclo-*t*-Bu<sub>4</sub>-Sb<sub>4</sub>.<sup>12</sup>

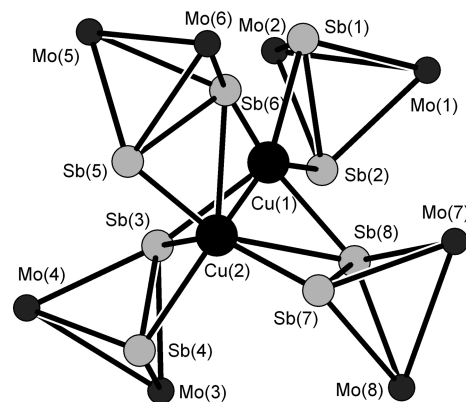
In contrast to the lighter analogues **2** and **3**, the CuI complex **4** forms a polymeric chain  $[\{\text{CpMo}(\text{CO})_2\}_2\text{Sb}_2(\text{CuI})]_\infty$  in the solid state. The polymer is built from two types of centrosymmetric dimeric arrangements,  $[\{\{\text{CpMo}(\text{CO})_2\}_2\text{Sb}_2\}_2(\text{CuI})_2]$ , similar to those observed in **2** and **3** (Figure 3). These alternating units are connected by Cu–I and Cu–Sb bonds forming the polymeric skeleton. Selected bond lengths and angles are summarized in Table 3.

The framework of the polymer consists of planar Cu<sub>2</sub>I<sub>2</sub> rhombs connected in a trans configuration by Cu–I bonds (Figure 4). The Cu–I bonds within the ring that provides the iodine to the extraannular Cu–I bonds [Cu(1)–I(1), Cu(1)–I(1'), av. = 2.63 Å] are marginally shorter than the Cu–I bonds within the ring that provides the copper to the extraannular Cu–I bonds [Cu(2)–I(2), Cu(2)–I(2'), av. = 2.69 Å], which in turn are shorter than the extraannular Cu–I bonds [2.7990(11) Å]. The intraannular Cu–I bond distances are comparable to the ones found in similar dimeric compounds:  $[(\text{Ph}_3\text{Sb})_2(\text{CuI})_2]$  [2.620(1)–2.640(1) Å]<sup>19</sup> and

**Figure 4.** Fragment from the linear polymeric framework of **4** in the crystal. The CO and Cp groups were omitted for clarity.

$[(2\text{-iodopyrazine-}N(\text{CuI}))_\infty]$  [2.627(1)–2.658(1) Å].<sup>22</sup> The Cu(1)···Cu(1') distance [2.6781(17) Å] is appreciably shorter than both the Cu(2)···Cu(2') distance [2.9745(18) Å] and the corresponding separation in **2** and **3** (av. = 2.94 Å). This is also reflected by the values observed for the Cu–I–Cu and I–Cu–I angles within the rings. The I(1) center is coordinated to three Cu atoms in a distorted trigonal pyramidal arrangement, with Cu–I–Cu bond angles in the range of 61.12(3)–109.90(4)°.

The coordination sphere of each Cu is completed by a  $[\text{CpMo}(\text{CO})_2\text{Sb}_2]$  ligand coordinating through both antimony atoms [Cu–Sb, 2.6237(10)–2.7335(13) Å]. In addition, a longer Sb–Cu bond [Cu(1)–Sb(3), 2.9361(14) Å] connects two consecutive Cu<sub>2</sub>I<sub>2</sub> units. In this fashion, each copper achieves a distorted trigonal bipyramidal coordination geometry, and in both cases, the equatorial plane coincides with the Cu<sub>2</sub>I<sub>2</sub> plane. The sum of the bond angles at copper in the equatorial plane are 359.17(4)° for Cu(1) and 352.76(4)° for Cu(2), and the bond angles at copper formed by the axial substituents are 146.95(4)° for Cu(1) and 158.36(4)° for Cu(2). As a general trend, it is observed that the equatorial bonds are notably shorter than the axial bonds. The only axial Cu–I bond, I(1)–Cu(2), is 0.14 Å longer than the average

**Figure 5.** View of the dication in **5**. The Cp and CO ligands were omitted for clarity.

**Table 4.** Selected Bond Lengths (Å) and Bond Angles (deg) for **5**

Cu(1)–Cu(2)	2.614(2)		
Sb(1)–Cu(1)	2.7327(18)	Sb(2)–Cu(1)	2.6610(17)
Sb(3)–Cu(1)	2.7117(18)	Sb(4)–Cu(2)	2.7350(18)
Sb(6)–Cu(1)	2.6845(17)	Sb(5)–Cu(2)	2.7683(17)
Sb(8)–Cu(1)	2.7204(18)	Sb(7)–Cu(2)	2.7836(17)
Sb(3)–Cu(2)	2.8698(17)	Sb–Sb	2.7382(12)–2.7672(13)
Sb(6)–Cu(2)	2.7618(18)	Mo–Mo	3.1003(16)–3.1476(19)
Sb(8)–Cu(2)	2.8037(17)	Sb–Mo	2.7443(13)–2.8912(14)
Sb(3)–Cu(1)–Sb(6)	104.58(6)	Sb(4)–Cu(2)–Sb(5)	104.43(5)
Sb(3)–Cu(1)–Sb(8)	99.15(6)	Sb(4)–Cu(2)–Sb(7)	104.30(6)
Sb(6)–Cu(1)–Sb(8)	102.05(6)	Sb(5)–Cu(2)–Sb(7)	103.75(5)
Sb(1)–Cu(1)–Sb(3)	124.99(6)	Sb(2)–Cu(1)–Sb(3)	92.63(6)
Sb(1)–Cu(1)–Sb(6)	90.59(6)	Sb(2)–Cu(1)–Sb(6)	152.31(7)
Sb(1)–Cu(1)–Sb(8)	129.32(7)	Sb(2)–Cu(1)–Sb(8)	96.29(6)
Sb(4)–Cu(2)–Sb(3)	58.43(4)	Cu(2)–Cu(1)–Sb(3)	65.18(5)
Sb(5)–Cu(2)–Sb(6)	59.51(4)	Cu(2)–Cu(1)–Sb(6)	62.81(5)
Sb(7)–Cu(2)–Sb(8)	58.81(4)	Cu(2)–Cu(1)–Sb(8)	63.37(5)
Sb(2)–Cu(1)–Sb(1)	61.72(4)	Cu(1)–Cu(2)–Sb(4)	114.09(7)
Cu(2)–Cu(1)–Sb(1)	153.34(8)	Cu(1)–Cu(2)–Sb(5)	115.08(7)
Cu(2)–Cu(1)–Sb(2)	144.86(8)	Cu(1)–Cu(2)–Sb(7)	113.94(7)

of the other Cu–I bonds. The axial Sb–Cu bonds (av. = 2.80 Å) are all longer than the equatorial Sb–Cu bonds (av. = 2.66 Å). The Sb–Cu bonds in complex **4**, containing pentacoordinated copper, are longer than the Sb–Cu bonds in **2** and **3** (av. = 2.57 and 3.60 Å, respectively), which contain tetraordinated copper centers. The Sb–Sb bonds of the Mo<sub>2</sub>Sb<sub>2</sub> ligands in **4** (av. Sb–Sb, 2.744 Å) are similar to those observed in **3** and are longer than those in the free Mo<sub>2</sub>Sb<sub>2</sub> ligand [Sb–Sb, 2.678(1) Å].<sup>2b</sup>

Polymer **4** is soluble in organic solvents, and the ESI-MS spectra obtained using these solutions display signals characteristic to [[CpMo(CO)<sub>2</sub>]<sub>2</sub>Sb<sub>2</sub>]<sub>2</sub>(CuI)<sub>2</sub> dimers. This suggests that the polymeric association is a solid-state phenomenon and that, in solution, oligomeric associates predominate.

The essential role of the halogen in the solid-state structures of **2**, **3**, and **4** led us to investigate the behavior of similar complexes containing a noncoordinating anion instead of a halogen. The diffusion-controlled reaction between [CpMo(CO)<sub>2</sub>]<sub>2</sub>Sb<sub>2</sub> in CH<sub>2</sub>Cl<sub>2</sub> and Cu[GaCl<sub>4</sub>] in benzene produced in 77% yield [[CpMo(CO)<sub>2</sub>]<sub>2</sub>Sb<sub>2</sub>]<sub>4</sub>Cu<sub>2</sub>[GaCl<sub>4</sub>]<sub>2</sub> (**5**) containing a dicationic cluster. The red crystalline air-sensitive solid has low solubility in hydrocarbons but is highly soluble in CH<sub>3</sub>CN. The IR spectrum of **4** displays stretching vibrations at 1888, 1899, 1911, 1941, 1967, and 2011 cm<sup>-1</sup>, corresponding to the CO ligands of the Mo<sub>2</sub>Sb<sub>2</sub> units. The heaviest ion observed in the ESI-MS spectrum was [[CpMo(CO)<sub>2</sub>]<sub>2</sub>Sb<sub>2</sub>]<sub>2</sub>Cu<sup>+</sup> at *m/z* = 1420.

The molecular structure of **5** was determined by single-crystal X-ray crystallography. The unit cell incorporates three benzene molecules for each cluster unit, and this composition was confirmed by elemental analysis. No contacts are observed between the two tetrachlorogallate counterions and the dicationic cluster.

The structure of the dicationic cluster in **5** is depicted in Figure 5, and selected bond lengths and angles are provided in Table 4. At the core of the structure there is a Cu–Cu dumbbell surrounded by three bridging Mo<sub>2</sub>Sb<sub>2</sub> ligands in a C<sub>3</sub>-symmetric propeller-like arrangement. The two quasi-equilateral triangles, Sb(3)Sb(6)Sb(8) and Sb(4)Sb(5)Sb(7),

are twisted with respect to each other by about 22.6°. The value of the Flack parameter [0.43(2)] did not allow for an assignment of the absolute configuration. A fourth Mo<sub>2</sub>Sb<sub>2</sub> ligand chelates Cu(1) with the Sb–Sb bond nearly perpendicular to the Cu–Cu axis. In the resulting structure, Cu(2) is hexacoordinated by antimony in a distorted trigonal prismatic arrangement, whereas the Cu(1) atom is pentacoordinated.

The Cu–Cu distance of 2.614(2) Å is shorter than in complexes **2** and **3** (av. = 2.94 Å) and also **4** (2.68 and 2.97 Å). For comparison, the Cu–Cu distance in Cu metal measures 2.556 Å.<sup>23</sup> The Cu–Cu separation in cluster **5** is intermediate in length between the Cu–Cu distances in tetrameric organocopper(I) compounds (RCu)<sub>4</sub> [e.g., R = C<sub>6</sub>F<sub>5</sub>, 2.4286(3)–2.4538(3) Å;<sup>24</sup> R = 2,4,6-*i*-Pr<sub>3</sub>C<sub>6</sub>H<sub>2</sub>, 2.445–(1),<sup>25</sup> R = Me<sub>3</sub>SiCH<sub>2</sub>, 2.42 Å],<sup>26</sup> and the sum of the van der Waals radii for copper (2.8 Å)<sup>23</sup> indicating a certain degree of Cu–Cu bonding interaction. The Sb–Cu(2) bonds [2.7350–(18)–2.8698(17) Å] are longer than the Sb–Cu(1) bonds [2.6610(17)–2.7327(18) Å], which is not surprising given the larger coordination number of Cu(2) versus Cu(1). For complexes **2**–**5**, a continuous increase in the Cu–Sb bond length from 2.56–2.61 Å for four-coordinated copper to 2.62–2.73 Å for five-coordinated copper and 2.73–2.86 Å for six-coordinated copper is noticeable.

The Sb–Sb bond lengths in **5** average 2.74 Å, practically identical to the ones observed in complexes **2**–**4**. Given the relatively large size of antimony, it is surprising that the preferred structure is not [[CpMo(CO)<sub>2</sub>]<sub>2</sub>Sb<sub>2</sub>]<sub>2</sub>Cu<sup>+</sup>, with the copper center in a tetrahedral environment. The stability of this moiety is suggested by the intense signal it generates in the mass spectra. The preference for the asymmetric cluster

(23) Wiberg, N. *Holleman-Wiberg Lehrbuch der Anorganischen Chemie*; Walter de Gruyter: Berlin, New York, 1995; p 1839.

(24) Sundararaman, A.; Lalancette, R. A.; Zakharov, L. N.; Rheingold, A. L.; Jäkle, F. *Organometallics* **2003**, *22*, 3526–3532.

(25) Nobel, D.; van Koten, G.; Spek, A. L. *Angew. Chem., Int. Ed. Engl.* **1989**, *28*, 208–210; *Angew. Chem.* **1989**, *101*, 211.

(26) Jarvis, J. A. J.; Pearce, R.; Lappert, M. F. *J. Chem. Soc., Dalton Trans.* **1977**, 999–1003.

(22) Nather, C.; Wriedt, M.; Jess, I. *Inorg. Chem.* **2003**, *42*, 2391–2397.

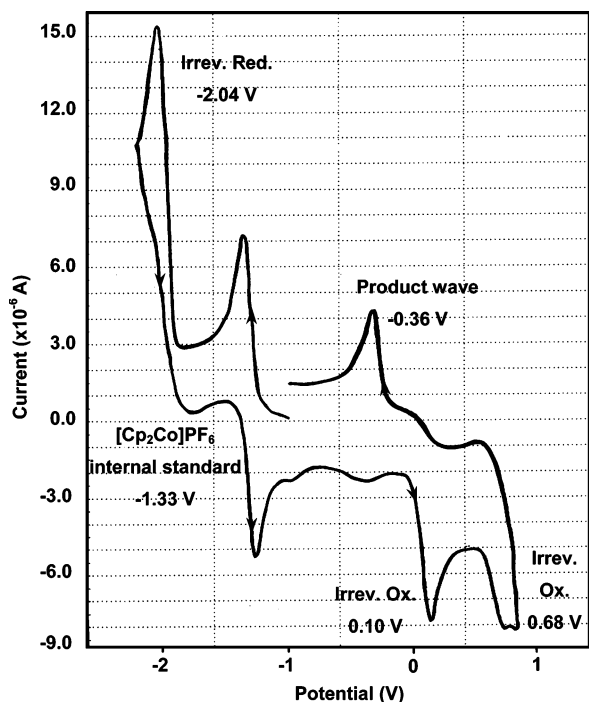


**Figure 6.** Cyclic voltammogram of **1** in dichloromethane at a scan rate of  $200 \text{ mV} \cdot \text{s}^{-1}$  in the presence of  $[\text{Cp}_2\text{Co}]\text{PF}_6$  as in internal standard. Values are given with respect to ferrocene.

in **5** is probably because of the higher coordination number of antimony in this structure and the strength of the Cu–Cu interaction.

Attempts to isolate copper(II) complexes containing **1** as a ligand resulted in the reduction of the metal and the isolation of copper(I) complexes. Silver(I) salts were reduced by **1** to metallic silver. A similar behavior has been described for the phosphorus analogue of **1**, [ $\{\text{CpMo}(\text{CO})_2\}_2(\mu, \eta^2\text{-P}_2)\}$ .<sup>8d</sup> A cyclic voltammogram in dichloromethane (Figure 6) revealed that **1** was irreversibly reduced at a peak potential of  $-2.04 \text{ V}$  and irreversibly oxidized at  $0.10 \text{ V}$  versus ferrocene. A second irreversible oxidation took place at a peak potential of  $0.68 \text{ V}$ . It is, therefore, not surprising that silver(I), with a reported formal potential in dichloromethane of  $0.65 \text{ V}$  versus ferrocene, was reduced to metallic silver.<sup>27</sup> This value is in good agreement with the known sensitivity of **1** toward air oxidation.

## Conclusion

Dimers, a polymer and a dicationic cluster containing the ligand **1** coordinated to copper(I), have been obtained by self-assembly and were crystallographically characterized. The study indicates that **1**, with its bite of about  $2.75 \text{ \AA}$ , prefers the chelate versus the bridging coordination mode for copper(I), and the  $[\text{CpMo}(\text{CO})_2]_2\text{Sb}_2\text{Cu}$  entity was prevalent in the described complexes. In contrast, its phosphorus analogue, with a bite of only  $2.08 \text{ \AA}$ , prefers to bridge two copper centers.<sup>8a,d</sup> When present as counterions, halogens assumed bridging positions between copper centers and were, therefore, incorporated in the skeleton of the resulting architecture. However, **1** proved its ability to assist the polymer creation through the formation of Sb–Cu bonds. In the absence of coordinating anions, **1** coordinated in both chelating and bridging fashions, supporting the formation of a Cu–Cu dumbbell. A cyclic voltammogram in dichloromethane showed that **1** was irreversibly oxidized at a potential of  $0.10 \text{ V}$  versus ferrocene and was, therefore, unsuitable for coordination to metals with higher formal potentials, such as silver(I). In light of this study, it appears tempting to investigate the coordination behavior of the related cluster  $[\text{CpMo}(\text{CO})_2\text{Sb}_3]$  and its ability to generate supramolecular architectures through self-assembly.

**Acknowledgment.** This work was supported by the Natural Sciences and Engineering Research Council of Canada, the Canada Foundation for Innovation, and the Alberta Science and Research Investments Program. We thank Dr. Warren Piers and Dr. David Emslie for support with the electrochemical measurements.

**Supporting Information Available:** Complete crystallographic data in table format. This material is available free of charge via the Internet at <http://pubs.acs.org>. CIF files are available on-line from the Cambridge Crystallographic Data Centre [CCDC nos. 281286 (2), 281287 (3), 281288 (4), and 281289 (5)].

IC051406L

- (27) (a) Connelly, N. G.; Geiger, W. E. *Chem. Rev.* **1996**, *96*, 877–910.  
(b) Song, L.; Troglor, W. C. *Angew. Chem., Int. Ed. Engl.* **1992**, *31*, 770–772.